

# Nucleic Acid Isolation: Fundamentals of Sample Preparation Methodologies, Current Advancements, and Future Endeavors

Miranda N. Emaus, Marcelino Varona, Derek R. Eitzmann, Shu-An Hsieh,  
Victoria R. Zeger, and Jared L. Anderson\*

Department of Chemistry, Iowa State University, Ames, Iowa United States

## 7 Abstract

The isolation of nucleic acids (NA) is an essential component of NA analysis. Without sufficient purification, contaminants co-existing with NAs often inhibit enzymatic amplification causing poor reproducibility and sensitivity. Numerous advancements in NA sampling in recent years have led to improvements in extraction yields from complex matrices and the reduction of analysis times. Perhaps most notably is the push towards miniaturization and automation to facilitate point-of-care testing. This article reviews the advancements and current trends in NA sample preparation including cell lysis and NA purification.

\*Corresponding Author:

Jared L. Anderson

18 Department of Chemistry

19 Iowa State University

20 1605 Gilman Hall

21 Ames, Iowa 5001

22 andersoj@jastate.edu

23

25      **1. Introduction**

26              Sample preparation has aided NA analysis in becoming the cornerstone of forensic,  
27      environmental, and clinical applications. Advancements in NA sampling has stemmed largely  
28      from improving the yield of NAs isolated, minimizing the amount of impurities co-extracted with  
29      NAs, decreasing sample preparation time and sample volumes, and moving towards point-of-care  
30      (POC) testing. One of the biggest challenges for NA sample preparation is the co-extraction of  
31      impurities as enzymatic detection methods, such as polymerase chain reaction (PCR) and  
32      sequencing, are highly sensitive to inhibitors often causing low sensitivities and false negatives.  
33      Therefore, ideal sample preparation methods must remove inhibitors to ensure accurate and  
34      reproducible results.

35              The two distinct steps involved in sample preparation are cell lysis and NA purification.  
36      Ideally, a cell lysis method will efficiently disrupt the cell membrane to free intracellular  
37      components without inhibiting downstream extraction and detection methods. Recent studies in  
38      cell lysis have focused on the development of novel lysing agents as well as the development of  
39      microfluidic chips for POC testing. Liquid-liquid extraction (LLE) and solid phase extraction  
40      (SPE) are among the most popular modes of NA extraction. These methods are highly diverse and  
41      utilize electrostatic, hydrophobic, or hydrogen bonding interactions to extract and preconcentrate  
42      NAs. Recent advances in NA extraction focus on limiting the sample volume and developing POC  
43      testing methods for analysis outside of traditional laboratory settings. One approach to furthering  
44      POC diagnostics is the development of microfluidic devices that integrate multiple sample  
45      preparation steps into a single chip. In addition, sequence-specific NA extractions are also vital to  
46      preconcentrate low abundance fragments in the presence of large amounts of background DNA.

47        Here, we provide a review of the most recent trends in cell lysis and NA extraction. We  
48    discuss the progress that has been made in the development of novel lysis procedures and  
49    extraction solvents/sorbents, strategies used to reduce contamination by PCR inhibitors, and the  
50    miniaturization and automation of NA sample preparation.

51

## 52    **2. Cell Lysis**

53        Cell lysis is often the first step in NA sample preparation. There are numerous chemical  
54    and mechanical lysis methods with each offering different advantages and disadvantages. For  
55    example, chemical lysis methods are simple and require little instrumentation. However, chemical  
56    lysis reagents can inhibit downstream bioanalytical detection methods such as PCR and membrane  
57    sensors.[1,2] In comparison, mechanical lysis methods are chemical-free but require additional  
58    instrumentation to implement. However, recent studies have reduced instrumentation by  
59    developing microfluidic devices.

### 60    *2.1 Chemical Cell Lysis*

61        Detergents such as 2-[4-(2,4,4-trimethylpentan-2-yl)phenoxy]ethanol (Triton X-100) or  
62    sodium dodecyl sulfate (SDS) solubilize the cell membrane and release intracellular components.  
63    Although detergents are effective at lysing cells, high lysis efficiencies are essential when low cell  
64    counts are available. Le et al. investigated using the non-ionic detergent  
65    octylphenoxyethoxyethanol (IGEPAL CA-630) in conjunction with bovine serum albumin  
66    (BSA) to lyse circulating tumor cells.[3] BSA enhanced the lysis efficiency approximately 4-fold  
67    compared to the detergent alone. A 0.3% IGEPAL CA-630 and 0.1% BSA lysis solution  
68    outperformed a commercial kit at low cell counts (10 and 100 cells) but performed worse at higher  
69    cell counts due to RNase degradation. Recently, Strijp and co-workers developed a two-step

70 chemical lysis method to isolate RNA and DNA from a single colorectal cancer cell.[4] This on-  
71 chip method utilized an initial 0.5x Tris/Borate/EDTA (TBE), 0.5% v/v Triton X-100 buffer to  
72 release RNA in the cytosol. The nuclear membrane was subsequently lysed to release DNA using  
73 a 0.5x TBE, 0.5% v/v Triton X-100, and protease K lysis solution.

74 Ionic liquids (ILs) are organic molten salts with melting temperatures under 100 °C.  
75 Altering their cation or anion can provide different physiochemical properties while promoting  
76 different interactions with analytes. Ressmann et al. reported screening 20 hydrophilic ILs for their  
77 ability to lyse animal tissue cells from meat samples.[5] The choline hexanoate ( $[\text{Chol}^+][\text{Hex}^-]$ ) IL  
78 significantly aided the lysis process. The 1-ethyl-3-methylimidazolium acetate ( $[\text{EMIM}^+][\text{OAc}^-]$ )  
79 and  $[\text{Chol}^+][\text{Hex}^-]$  ILs have more recently been used to lyse gram-positive and negative bacteria.  
80 Gram-positive bacteria are difficult to lyse due to a thick peptidoglycan layer and require more  
81 stringent lysis conditions, such as lysozyme treatment or sonication.[6] However, the  
82  $[\text{EMIM}^+][\text{OAc}^-]$  and  $[\text{Chol}^+][\text{Hex}^-]$  ILs were remarkably capable of effectively lysing four gram-  
83 positive bacteria in 5 min with mild heating at 65 °C.

84 Fuchs-Telka et al. employed hydrophobic ILs to lyse gram-negative bacteria.[7]  
85 Dissolution of the 1-butyl-1-methylpyrrolidinium bis[(trifluoromethyl)sulfonyl]imide  
86 ( $[\text{BMPyr}^+][\text{NTf}_2^-]$ ) IL was shown to not significantly inhibit quantitative PCR (qPCR), and with  
87 mild heating could lyse over 88% of gram-negative cells in 1 min. However, the  $[\text{BMPyr}^+][\text{NTf}_2^-]$   
88 IL only lysed 5% of gram-positive cells. Further optimization of the IL structure could effectively  
89 lyse gram-positive cells in the same amount of time. Hydrophobic ILs have also been applied  
90 towards the lysis of viruses and subsequent extraction of viral RNA and DNA.[8] The IL-based  
91 method generally obtained better results with DNA viruses compared to RNA viruses. However,

92 the 1,3-dimethylimidazolium methylphosphonate IL extracted 244% more RNA compared to a  
93 commercial kit.

94 Electrochemical lysis uses a localized high pH generated by a cathode to disrupt the cell  
95 membrane. Compared to traditional electrical lysis methods, electrochemical lysis requires lower  
96 voltages and avoids joule heating, which can lead to bubble formation. Wang et al. devised the  
97 electrochemical lysis device illustrated in Figure 1 to lyse gram-negative and gram-positive  
98 bacteria.[9] Cell death was noted visually in 30 s. However, a 1 min lysis step was optimum and  
99 provided an 8-cycle improvement by qPCR after subsequent DNA purification.

100 *2.2 Mechanical Cell Lysis*

101 Mechanical lysing methods such as freeze/thaw, bead beating, surface acoustic waves  
102 (SAW), and electrical lysis are effective chemical-free lysis methods. Recent studies have  
103 integrated mechanical lysis methods into microfluidic chips, thereby reducing the amount of  
104 equipment needed and providing an automated method.

105 Bead beating lysis methods utilize small (~100  $\mu\text{m}$ ), inert beads to induce mechanical shear  
106 on cells. Berasaluce et al. developed a continuous flow microfluidic device to lyse gram-positive  
107 bacteria using zirconium/silica beads.[2] The quantity and size of beads inside the lysis chamber  
108 had a significant effect on the probability of the beads colliding with cells. However, too many  
109 small beads were observed to clog the channel or hinder the rotation of the magnet. Yan and co-  
110 workers used zirconia beads to lyse gram-negative and gram-positive bacteria followed by loop-  
111 mediated isothermal amplification (LAMP) on a centrifugal chip.[10] Only 70 minutes were  
112 required from the injection of the bacteria to detection with a limit of detection as low as 10 CFU  
113  $\mu\text{L}^{-1}$ .

114 Kamat et al. utilized mechanical vibrations and chitosan-coated magnetic nanoparticles to  
115 lyse six gram-negative pathogens on a microfluidic chip.[11] Frequencies above 150 Hz were  
116 capable of inducing cell lysis whereas frequencies above 240 Hz resulted in DNA damage. The  
117 nanoparticles aided in improving cell lysis by colliding with cells and imparting mechanical stress.  
118 Once lysed, the chitosan-coated nanoparticles captured DNA through electrostatic interactions.

119 SAWs are Rayleigh waves generated on a piezoelectric crystal surface stimulated from a  
120 radio frequency. When the SAW encounters a droplet containing a cell suspension, lysis occurs  
121 due to acoustic pressure imparting mechanical stress. Taller et al. utilized SAWs to lyse exosomes  
122 and detect microRNA (miRNA) using an ion-exchange nanomembrane.[12] The lysis efficiency  
123 was only 38%, but the lysis step did not deleteriously affect the nanomembrane. Wang et al. added  
124 polystyrene (PS) microparticles to a suspension of breast cancer cells to improve the lysis  
125 efficiency using SAW.[13] Collisions of the microparticles with the cells greatly improved the  
126 lysis efficiency from 44% (without microparticles) to 92% (with microparticles).

127 Electrical lysis functions by creating pores in the cell membrane and causing irreversible  
128 damage at high voltages.[9,14] Gross et al. developed a 3D-printed fluidic device to electrically  
129 lyse adhered endothelial cells.[15] The device was modified with poly(dimethylsiloxane) or PS to  
130 capture cells, and a 500 V power source allowed for lysis efficiencies as high as 96%. However,  
131 electrical cell lysis generally requires high voltages to efficiently lyse cells, which can be  
132 problematic when coupling to microfluidic chips as joule heating and bubble formation can occur.  
133 Gabardo et al. developed 3D multi-scale electrodes that lowered the required potential to only 4  
134 V.[14] The 3D multi-scale electrodes produced over 95% lysis efficiencies by reducing inter-  
135 electrode separation and incorporating nanoscale materials, such as gold film, onto the electrode  
136 surface.

137 **3. Liquid-Liquid Extraction**

138 LLE utilizes two immiscible solvents to concentrate analytes in one of the phases. Early  
139 NA LLE approaches, such as phenol-chloroform LLE, utilized volatile organic solvents and  
140 required numerous sample handling steps. To reduce the use of volatile solvents, NA extractions  
141 have been miniaturized to require microliter or milliliter volumes. Recently, novel extraction  
142 solvents such as deep eutectic solvents (DES), coacervates, and magnetic ionic liquids (MILs)  
143 have been implemented to purify NAs from complex matrices.

144 *3.1 Aqueous Biphasic Systems*

145 Aqueous biphasic systems (ABS) form between two water-miscible solutes that are  
146 immiscible under critical conditions. Phase formation occurs when interactions between the solute  
147 molecules are more favorable than interactions with water. Zhang et al. developed an ABS  
148 containing one of 16 novel quaternary ammonium salts and polyethylene glycol (PEG)-based  
149 DESs to extract RNA.[16] DESs consist of a hydrogen bond donor and acceptor that form a  
150 homogenous mixture with a lower melting temperature than the individual components.  
151 Tryptophan was spiked into the RNA sample to assess the co-extraction of proteins with DNA.  
152 Extraction efficiencies of over 92% were achieved for both RNA and tryptophan, but only 27.02%  
153 and 86.19% of tryptophan and RNA, respectively, were recovered from the DES providing an  
154 interesting method for purifying NAs. Similarly, Xu et al. used a two-phase system comprised of  
155 ILs and DESs to extract salmon testes DNA.[17] The trimethylglycine formate IL performed the  
156 best with an extraction efficiency of 95.86%. When examining the co-extraction of cytochrome c  
157 (Cyt-c) and bovine hemoglobin (BHb), nearly 100% DNA was found in the IL phase whereas only  
158 1.86% and 45.59% of Cyt-c and BHb, respectively, was identified in the IL phase. Differential

159 partitioning of DNA and two proteins was dependent on the isoelectric point of the biomolecules,  
160 suggesting that pH modification could be exploited to isolate DNA from PCR inhibitors.

161 Bio-based ILs often contain an amino acid or carbohydrate-based anion. Therefore, bio-  
162 based ILs are considered more environmentally-friendly compared to traditional classes of ILs.  
163 Quental et al. demonstrated that amino acid-based ILs can form ABSs with polypropylene glycol  
164 (PPG) and quantitatively extract RNA.[18] The  $[\text{Chol}^+]$  L-glutamate and  $[\text{Chol}^+]$  L-aspartate ILs  
165 preserved RNA for up to 15 days, with the  $[\text{Chol}^+]$  L-aspartate IL also preventing RNase  
166 degradation. However, in a bacterial lysate, residual RNA was found in the PEG along with co-  
167 extracted DNA. Additional optimization of the mixture composition or operational conditions has  
168 the potential to reduce matrix effects and co-extraction of DNA.

169 To reduce the number of sample handling steps, Cheung et al. combined Triton X-100 ABS  
170 with thermophilic helicase dependent amplification (tHDA) to isolate and amplify DNA from *E.*  
171 *coli* in a one-step procedure.[19] After lysing the cells in the detergent phase, DNA migrated to  
172 the tHDA buffer phase where it was amplified. This method has the potential for POC diagnostics  
173 if visual detection is utilized as only a heat block would be required for analysis.

174 *3.2 Coacervate Separation*

175 Polyelectrolytes can form liquid droplets known as coacervates permitting phase separation  
176 between the aqueous and solute-rich phase. Frankel et al. generated the coacervates, shown in  
177 Figure 2, to capture RNA via ion-exchange.[20] Coacervates used were comprised of  
178 poly(allylamine hydrochloride, three adenine nucleotides (5'-AMP, 5'-ADP, and 5'-ATP), and  
179  $\text{Mg}^{2+}$ . RNA extractions from complex matrices using coacervates were not examined, and future  
180 studies should examine extraction from different matrices to assess the method's practicality.

181     3.3 *Membrane Separation*

182           Membrane separations have been applied for the preconcentration of DNA and proteins  
183   using DESs as draw solutions.[21] Using forward osmosis, the feed solution is passed through the  
184   membrane into the draw solution leaving larger analytes to collect within the feed solution. A thin-  
185   film composite polyamide membrane hindered the flux of DNA and proteins into the choline  
186   chloride and ethylene glycol DES draw solution. Enrichment factors greater than 3 and 6 for DNA  
187   and BSA, respectively, were achieved while maintaining the integrity of biomolecules.

188     3.4 *Liquid-Liquid Microextraction*

189           Liquid-liquid microextractions revolve around using only microliter volumes of extraction  
190   solvents to efficiently isolate analytes and minimize solvent waste. Clark et al. demonstrated the  
191   first DNA extraction with three hydrophobic MILs.[22] MILs are a subclass of ILs containing a  
192   paramagnetic component allowing droplets to respond to an external magnetic field. Extraction  
193   efficiencies over 90% were obtained by dispersing the trihexyl(tetradecyl)phosphonium  
194   tetrachloroferrate(III) ( $[P_{66614}^+][FeCl_4^-]$ ) MIL. However, the benzyltriocetylammonium  
195   bromotrichloroferrate(III) ( $[(C_8)_3BnN^+][FeBrCl_3^-]$ ) MIL extracted significantly less albumin  
196   compared to the other Fe(III)-based MILs demonstrating that altering the MIL structure can have  
197   a significant effect on the extraction of impurities. Emaus et al. investigated the effect of the  
198   paramagnetic metal center of acetylacetone-based MILs on DNA extraction.[23] The nickel-  
199   based MIL produced 4-6 times higher enrichment factors compared to the cobalt and dysprosium-  
200   based MILs. In addition, the manganese-based MIL poorly extracted DNA compared to the Ni-,  
201   Co-, or Dy-based MILs. Desorbing DNA from either a liquid solvent or solid sorbent can be time-  
202   consuming and is often incomplete. Therefore, Emaus et al. integrated DNA-enriched MILs into

203 custom-designed qPCR buffers to thermally desorb DNA during qPCR without impacting the  
204 amplification efficiency.

205 **4. Solid Phase Nucleic Acid Extraction**

206 The extraction of NAs using solid sorbents is a promising area of research capable of  
207 isolating NAs with limited use of organic solvents. Silica-based techniques comprise most  
208 commercially-available SPE kits. These kits use chaotropic salts to disrupt the solvation of the  
209 biopolymer and facilitate the adsorption of NAs. Adsorbed NAs are then washed with alcohol  
210 and eluted with a low ionic strength solvent. Recent work by Günal et al. compared the DNA  
211 extraction behavior of silica microspheres of varying pore sizes and polymer coatings.[24]  
212 Monodisperse silica particles extracted more DNA when silica gel possessed a bimodal  
213 distribution of pore sizes due to an increased surface area and rate of mass transport.

214 Juang et al. developed a method called centrifugation-assisted immiscible fluid filtration  
215 (CIFF) to extract DNA and messenger RNA (mRNA).[25] As shown in Figure 3, dehydrated  
216 NAs were adsorbed to the microbeads, followed by pelleting of the beads in a fluorinated oil to  
217 isolate NAs from impurities. This method allows for the high-throughput analysis of NAs  
218 without manual wash steps, thereby reducing the risk of contamination. CIFF was successfully  
219 able to isolate enough DNA for qPCR detection from 10 cancer cells with only 0.5% carryover  
220 from the sample solution.

221 *4.1 Magnetic Nanoparticles*

222 Traditional silica-based extraction platforms require specialized equipment and  
223 significant user intervention. In comparison, magnetic nanoparticles only require an external

224 magnet to recover DNA-enriched particles. Magnetic nanoparticles are also attractive due to  
225 their large surface area and ease of modification.

226 Bare iron magnetic nanoparticles are easily oxidized and have low affinity for NAs.  
227 Therefore, studies have evaluated coating magnetic nanoparticles to improve their affinity for  
228 NAs. Nanayakkara et al. implemented chitosan-coated iron nanoparticles to extract genomic  
229 DNA from whole blood.[26] The particles lysed white blood cells through bead beating while  
230 simultaneously adsorbing DNA. The DNA-enriched nanoparticles were added to a qPCR buffer  
231 to bypass a time-consuming desorption step. Hu et al. coated iron phosphate nanoparticles with  
232 polyethyleneimine and demonstrated its ability to extract 4.6  $\mu$ g of genomic DNA from whole  
233 blood via electrostatic interactions at pH 4.[27] Nearly 80% of extracted DNA could be  
234 recovered by increasing to a pH of 10. Haddad et al. examined the physical characteristics of  
235 different coatings through the measurement of particle size and zeta potential before and after  
236 DNA binding.[28] Silica and tripolyphosphate functionalized particles exhibited zeta potentials  
237 of  $+5.55 \pm 2.10$  and  $+1.78 \pm 1.73$  mV, respectively. The tripolyphosphate magnetic particles  
238 possessed a lower zeta potential but extracted 100-fold more DNA than the silica particles. Bai et  
239 al. developed a method using amine-rich silica-coated iron oxide nanoparticles for NA  
240 isolation.[29] The amine-rich coating greatly increased the surface area of the particles and was  
241 directly added to the PCR buffer for successful amplification.

242 Magnetic nanoparticles have also been widely used as composite extraction phases to  
243 recover the extraction phase. Xu et al. utilized chitosan-modified iron-magnetized multi-walled  
244 carbon nanotubes coated with a PEG-based DES to extract up to 178 mg of DNA per gram of  
245 sorbent.[30]. In comparison, the composite could only load up to  $15 \text{ mg g}^{-1}$  of BHb. Liu et al.  
246 developed a DNA extraction phase consisting of reduced graphene oxide, chitosan-

247 functionalized magnetic nanoparticles, and a guanidinium-based IL.[31] This phase extracted  
248 233 mg of salmon testes DNA per gram of sorbent while extracting less than 5% of BHb. Meng  
249 et al. utilized magnetic nanoparticles functionalized with a metal-organic framework dispersed in  
250 a lactic acid-based DES to extract RNA.[32] The composite was able to selectively extract RNA  
251 over DNA, Cyto-c, tryptophan, and tyrosine through chelation, electrostatic, hydrophobic, and  
252 hydrogen bonding interactions. Yan et al. employed a reduced graphene oxide phase combined  
253 with magnetic nanoparticles to isolate miRNAs.[33] The material preferentially extracted  
254 miRNA over mRNA due to the larger diffusivity of miRNA.

255 *4.2 Polymeric Ionic Liquid Sorbents*

256 Solid-phase microextraction (SPME) utilizes a fiber coated with a sorbent for solventless,  
257 non-exhaustive preconcentration of analytes. SPME is a unique extraction method as it does not  
258 require significant instrumentation to extract or recover analytes, making it ideal for POC testing.  
259 Nacham et al. used a polymeric ionic liquid (PIL) sorbent coating for DNA and yeast RNA  
260 extractions.[34,35] PILs are polymers produced from the polymerization of IL monomers that  
261 retain many properties of ILs (i.e., thermal stability and structural tunability). NAs were  
262 extracted by the coating through anion exchange. Varona et al. expanded the use of the PIL  
263 fibers to isolate DNA from lysed *Mycobacteria smegatis* in an artificial sputum matrix.[36] To  
264 avoid diluting recovered DNA, a custom LAMP buffer was developed to allow direct addition of  
265 the desorption solution (1 M NaCl). This buffer was used along with hydroxy-naphthol blue [36]  
266 and sequence-specific molecular beacons for sequence-specific DNA detection.[37] With  
267 isothermal DNA amplification, the PIL-SPME procedure can be implemented in non-traditional  
268 laboratory settings for rapid and specific diagnostics.

269 **5. Microfluidic-based Nucleic Acid Extraction**

270 POC testing is capable of rapidly obtaining results at, or near, the sampling location.  
271 Traditional NA extraction techniques are not applicable for POC diagnostics due to numerous  
272 sample handling steps and the required instrumentation. Microfluidic systems rectify the  
273 limitations of conventional extraction methods by reducing sample volumes, improving  
274 portability, and allowing for automation by integrating multiple sample preparation steps into a  
275 single device.

276 *5.1 Magnetic Separation in Microfluidics*

277 The use of a magnetic field to transport and isolate NAs has been widely explored due to  
278 its potential for automation. Deraney and co-workers devised a synergistic method that integrated  
279 magnetic and electroosmotic forces in their microfluidic system to transport DNA-enriched silica-  
280 based magnetic beads within the chip.[38] Utilizing electroosmotic flow improved the DNA  
281 extraction yield 15% while the carryover volume was minimized to only 0.22%. Zhang et al. used  
282 a magnetic field to adhere silica-based magnetic beads to a coaxial channel. [39] Compared to  
283 traditional hollow channels, the coaxial channels allowed for higher DNA extraction efficiencies  
284 (~99%) potentially due to a greater surface area. Perez-Toralla et al. used magnetic microparticles  
285 to electrostatically extract DNA followed by digital droplet PCR from serum samples of cancer  
286 patients.[40] Extraction efficiencies were found to be significantly reduced when serum samples  
287 were used.

288 Strohmeier and co-workers integrated the lysis and extraction steps on a single centrifugal  
289 microfluidic LabDisk.[41] The chip contained silica-based magnetic beads to capture NAs from  
290 lysed white blood cells, *B. subtilis*, *E. coli*, and Rift Valley fever viruses. The beads were  
291 transferred between chambers using a magnetic field. The LabDisk extracted approximately 3-fold  
292 less DNA from whole blood compared to Qiagen spin columns. In addition, on-disk DNA

293 extraction suffered from up to 5.5% (w/v) ethanol co-extraction due to the limited ability of drying  
294 the beads within the chip. Ethanol can precipitate DNA as well as enzymes used in PCR. Therefore,  
295 further work should explore approaches that reduce ethanol co-elution.

296 *5.2 Filter-based Isolation using Microfluidics*

297 Filters present a simple yet customizable NA extraction method as the pore size, filter  
298 length, and coating can be easily modified for use in microfluidic devices. Brassard and co-workers  
299 utilized glass microfiber filters to extract DNA on a centrifugal chip.[42] Pneumatic pumping flow,  
300 which utilizes pressure ports to compress air and facilitate airflow through the channels, was  
301 integrated into the chip to reduce ethanol co-elution. A 10 min pneumatic pumping flow step  
302 reduced the amount of ethanol co-elution 10-fold, which is a significant improvement from  
303 Strohmeier et al.[41] The centrifugal microfluidic device extracted similar amounts of DNA  
304 compared to commercial spin columns.

305 Gan and co-workers inserted a chitosan-modified filter paper into the microchip shown in  
306 Figure 4.[43] The filter was able to extract 95% of DNA in a sample through electrostatic  
307 interactions and entanglement of DNA with the fiber matrix. An “*in situ*” PCR method was  
308 employed permitting DNA amplification within the extraction chamber without a desorption step.  
309 “*In situ*” PCR reduced the analysis time by removing a lengthy desorption step while simplifying  
310 the design of the microfluidic device.

311 *5.3 Channel Modifications*

312 Channels within a microfluidic chip provide a large surface area to extract NAs. Therefore,  
313 ample research has focused on modifying the channel for NA extractions. Jin and co-workers  
314 modified the channel wall with primary amines to capture dimethyl pimelimidate (DMP)-bound

315 NAs through the formation of amidine bonds.[44] DMP captured NAs through electrostatic  
316 interactions with DNA were released at high pH (pH>10). Compared to commercial spin columns,  
317 the microfluidic method extracted 8-fold less DNA. However, the major advantage of the DMP  
318 extraction method is its ability to remove 99% of proteins from the sample; further modification  
319 to the chip's design could help to improve the extraction efficiency. Kastania et al. utilized  
320 carboxylic acid modifications to the channel wall to extract NAs precipitated using PEG, ethanol,  
321 and sodium chloride.[45] A recovery efficiency of 96% was achieved.

322 *5.4 Paper-based Extraction Methods*

323 Paper-based microfluidic devices have garnered significant attention due to their low cost,  
324 portability, and disposability. Rodriguez et al. designed a paper-based platform for the isolation,  
325 isothermal amplification, and lateral flow detection of DNA.[46] DNA was precipitated in the  
326 sample port while aqueous waste was wicked through a membrane. Once purified, LAMP was  
327 performed in the sample port to amplify DNA within 30 min. The paper-based method was prone  
328 to false positives attributed to the self-priming of LAMP primers. To reduce the occurrence of  
329 false positives, sequence-specific probes can be employed.

330 **6. Sequence-Specific Nucleic Acid Extractions**

331 Target NA sequences often comprise a small fraction of the total NA population. To enable  
332 accurate detection and quantification of low abundance sequences, it is often necessary to include  
333 an enrichment step. NAs possess the ability to recognize complementary sequences through  
334 Watson-Crick base-pairing interactions. These specific interactions are often exploited to isolate  
335 specific sequences from complex samples. Short oligonucleotide probes are commonly used to

336 hybridize with target sequences. These probes are modified with functional groups (e.g., biotin)  
337 allowing them to be captured by a support possessing an affinity for the tag.

338 *6.1 Solid Supports for DNA Analysis*

339 Magnetic nanospheres were synthesized in a layer-by-layer fashion by Wen et al. to capture  
340 hepatitis B DNA.[47] The carboxylated nanospheres were functionalized with a streptavidin  
341 coating and modified with a biotin-labeled oligonucleotide complementary to a sequence in the  
342 HBV genome. Capture efficiencies as high as  $87\pm1.7\%$  were achieved using this approach.  
343 Daggumati et al. developed a method for the sequential detection and purification of specific NA  
344 sequences from complex biological samples using modified nanoporous gold electrodes.[48] The  
345 electrodes were modified with thiolated 26-mer DNA probes. After the hybridization and wash  
346 step, the newly formed duplex could be desorbed using cyclic voltammetry. The applied voltage  
347 (from 0 to -1.5 V) was successfully able to cleave the gold-thiol bond and prevent re-adsorption  
348 of the duplex.

349 An interesting approach was developed by Leslie et al. that allowed for the label-free,  
350 visual detection of DNA using paramagnetic bead aggregation.[49] In the presence of DNA and a  
351 rotating magnetic field, silica-coated magnetic particles underwent visual aggregation. This  
352 approach was developed further to enable the sequence-specific detection of a clinically-relevant  
353 *KRAS* mutation.[50] Single-nucleotide polymorphism (SNP) detection was achieved by  
354 functionalizing a portion of the beads with a stabilizing probe complementary to a conserved  
355 region, while the remaining beads were modified with a shorter discriminating probe  
356 complementary to the wild-type, as illustrated in Figure 5a. In the presence of the wild-type  
357 sequence, the discriminating probe was able to bind resulting in visual aggregation (Figure 5b).  
358 Conversely, when the mutant sequence was present, the discriminating probe was unable to bind

359 which prevented aggregation (Figure 5c). The wild-type sequence was detected in 2 min when  
360 placed in a 1:1 ratio with the mutant sequence.

361 *6.2 Selective DNA analysis using Liquid Supports*

362 While magnetic beads are a popular platform for sequence-specific enrichment, they suffer  
363 from aggregation and sedimentation which can lower extraction efficiencies. Recently, Clark et al.  
364 developed a method relying on the  $[P_{6,6,6,14}^+]$  tris(hexafluoroacetylacetato)manganate(II)  
365 ( $[Mn(hfacac)_3^-]$ ) MIL as a support for the sequence-selective capture of DNA.[51] Ion-tagged  
366 oligonucleotides (ITOs) possessing an affinity for the MIL were synthesized using thiol-ene  
367 “click” chemistry between a thiol-modified oligonucleotide and an allylimidazolium IL. A 1000-  
368 fold greater amount of DNA was extracted from a 16.9 fmol solution using a modified oligo  
369 compared to using an unmodified oligo.

370 Maruyama et al. developed a different approach to enable sequence-specific DNA  
371 extraction of short sequences using oleoyl-modified DNA probes.[52] These probes hybridized to  
372 their target and formed reverse micelles with dilauroylphosphatidylcholine and 1-hexanol to  
373 enable partitioning into an organic phase. A subsequent study demonstrated the sequence-selective  
374 extraction of an aptamer using this strategy.[53] It was shown that the aptamer was capable of  
375 recognizing its target following the extraction and back-extraction processes, revealing that the  
376 method maintains the structural integrity of the target DNA. The method was also expanded for  
377 the extraction of short RNA sequences.[54] However, this technique is limited to short sequences  
378 and required long analysis times, reducing its practicality.

379 *6.3 mRNA Analysis*

380        The analysis of mRNA is of significant interest due to its role in gene expression. mRNA  
381    possesses a poly-adenosine tail on its 3' end that prevents it from being enzymatically degraded in  
382    the cytoplasm. This portion of the mRNA molecule can serve as a molecular handle for sequence-  
383    specific extractions with oligonucleotide probes containing consecutive thymine bases. Nacham  
384    et al. developed a SPME sorbent using commercially-available polyacrylate (PA) fibers.[35] The  
385    PA fibers were modified with oligo deoxythymine 20 (dT<sub>20</sub>) for the selective extraction of mRNA.  
386    Successful analysis of mRNA using RT-qPCR was performed from a suspension of  $3.5 \times 10^7$  *S.*  
387    *cerevisiae* cells mL<sup>-1</sup>.

388        Scherp et al. developed a similar method called solid phase gene extraction (SPGE).[55]  
389    Pulled borosilicate glass rods were used to create needles that were subsequently modified  
390    with oligo-dT<sub>10</sub> nucleotides for selective mRNA extraction. Extractions were performed  
391    from *Drosophila* eggs and embryonic flax roots and provided unique spatial resolution. One  
392    drawback to the SPGE method was the brittle glass needles used as the support. Park et al.  
393    improved the method by generating SPGE probes using stainless steel acupuncture needles to  
394    generate a more robust support. These probes were used to analyze *Brassica* roots in two different  
395    studies.[56,57] More recently, Nestorova et al. interfaced SPGE with a lab-on-a-chip device for  
396    the seamless extraction and desorption of mRNA for RT-qPCR analysis.[58] The method analyzed  
397    mRNA from rat glioblastoma cell spheroids in 7 min.

398        Drop-seq is a popular technique for gene expression analysis permitting the capture,  
399    amplification, and barcoding of the transcriptome for individual cells. Next-generation sequencing  
400    is subsequently used to reveal the gene expression profile of each cell. However, these techniques  
401    are limited to information near the poly-A tail. Hanson et al. developed DNA barcoded beads  
402    capable of capturing the T-cell receptor  $\alpha$  and  $\beta$  chain mRNAs using a reversible chain blocking

403 group.[59] This allowed for the development of individual beads capable of simultaneously  
404 capturing two different sequences. The ability to obtain paired information for two mRNA  
405 sequences can be potentially useful in understanding various disease states.

406 *6.4 Sequence-Specific Nucleic Acid Capture for Proteomic Analysis of Bound Protein*

407 The analysis of proteins associated with chromatin and RNA is of significant interest in  
408 developing an in-depth understanding of gene expression and regulation. One method that has  
409 been developed to understand these proteins is called hybridization capture of chromatin-  
410 associated proteins for proteomics (HyCCAPP).[60] This approach uses DNA oligonucleotides  
411 bound to magnetic beads to capture specific chromosomal loci for LC-MS/MS analysis of the  
412 bound protein. This method relies on formaldehyde crosslinking of chromatin and subsequent  
413 capture of specific loci using magnetic beads. DNA oligonucleotides modified with desthiobiotin  
414 were used as capture probes to enable the detection of low-abundance proteins, as biotin-labeled  
415 probes produced a higher background. In a separate study, a multiplexed approach was developed  
416 to capture the 25S rDNA, ARX1, CTT1, and RPL30 genes from yeast and subsequently analyze  
417 the bound protein.[61] This was done using strand-displacement probes that enabled the selective  
418 displacement of each gene-protein pair for mass spectrometric analysis. This allowed for the  
419 capture of all sequences on individual beads, which significantly decreased the analysis time. A  
420 similar approach was utilized by Spiniello et al. for the study of proteins associated with specific  
421 long noncoding RNA sequences.[62]

422 **7. Conclusion and Future Outlook**

423 Recent advancements in NA sample preparation have improved the recovery of pure NAs  
424 while reducing the time required for sample preparation. The co-extraction of potential PCR

425 inhibitors has been minimized through the use of new NA extraction phases such as DESs, MILs,  
426 and magnetic composites. A move towards automation has also occurred by integrating sample  
427 preparation steps in microfluidic devices.

428 While continual efforts towards ensuring NA purity from increasingly more complex  
429 samples are needed, future endeavors should also focus on improving detection limits. Sequence-  
430 specific extractions have aided this goal by enriching low abundance mutations that would  
431 otherwise be masked during PCR. Enhanced NA preconcentration has the potential to be achieved  
432 by using lower desorption volumes or by integrating NA-enriched sorbents/solvents into a PCR  
433 assay to circumvent diluting recovered DNA. In addition, modifying the design of microfluidic  
434 chips has the potential to improve NA enrichment while still permitting POC testing. Lower  
435 detection limits will aid clinical and forensic applications by reducing the amount of sample  
436 required for analysis or permitting earlier detection of diseases through the analysis of viral NA or  
437 circulating tumor DNA.

438 **Acknowledgements:** The authors acknowledge funding from the Chemical Measurement and  
439 Imaging Program at the National Science Foundation (Grant No. CHE-1709372)

440

441

442

443

444

445

446

447

448 **8. References**

449 [1] C. Schrader, A. Schielke, L. Ellerbroek, R. Johne, PCR inhibitors - occurrence, properties  
450 and removal, *J. Appl. Microbiol.* 113 (2012) 1014–1026. doi:10.1111/j.1365-  
451 2672.2012.05384.x.

452 [2] A. Berasaluce, L. Matthys, J. Mujika, M. Antoñana-Díez, A. Valero, M. Agirregabiria,  
453 Bead beating-based continuous flow cell lysis in a microfluidic device, *RSC Adv.* 5  
454 (2015) 22350–22355. doi:10.1039/c5ra01251a.

455 [3] A.V.P. Le, D. Huang, T. Blick, E.W. Thompson, A. Dobrovic, An optimised direct lysis  
456 method for gene expression studies on low cell numbers, *Sci. Rep.* 5 (2015) 1–10.  
457 doi:10.1038/srep12859.

458 [4] D. Van Strijp, R.C.M. Vulders, N.A. Larsen, J. Schira, L. Baerlocher, M.A. Van Driel, M.  
459 Pødenphant, T.S. Hansen, A. Kristensen, K.U. Mir, T. Olesen, W.F.J. Verhaegh, R. Marie,  
460 P.J. Van Der Zaag, Complete sequence-based pathway analysis by differential on-chip  
461 DNA and RNA extraction from a single cell, *Sci. Rep.* 7 (2017) 1–9. doi:10.1038/s41598-  
462 017-10704-4.

463 [5] A.K. Ressmann, E.G. García, D. Khlan, P. Gaertner, R.L. Mach, R. Krska, K. Brunner, K.  
464 Bica, Fast and efficient extraction of DNA from meat and meat derived products using  
465 aqueous ionic liquid buffer systems, *New J. Chem.* 39 (2015) 4994–5002.  
466 doi:10.1039/c5nj00178a.

467 [6] M. Mahalanabis, H. Al-Muayad, M.D. Kulinski, D. Altman, C.M. Klapperich, Cell lysis  
468 and DNA extraction of gram-positive and gram-negative bacteria from whole blood in a  
469 disposable microfluidic chip, *Lab Chip.* 9 (2009) 2811–2817. doi:10.1039/b905065p.

470 [7] S. Fuchs-Telka, S. Fister, P.J. Mester, M. Wagner, P. Rossmanith, Hydrophobic ionic  
471 liquids for quantitative bacterial cell lysis with subsequent DNA quantification, *Anal.  
472 Bioanal. Chem.* 409 (2017) 1503–1511. doi:10.1007/s00216-016-0112-x.

473 [8] S. Fister, S. Fuchs, P. Mester, I. Kilpeläinen, M. Wagner, P. Rossmanith, The use of ionic  
474 liquids for cracking viruses for isolation of nucleic acids, *Sep. Purif. Technol.* 155 (2015)  
475 38–44. doi:10.1016/j.seppur.2015.03.035.

476 [9] S. Wang, Y. Zhu, Y. Yang, J. Li, M.R. Hoffmann, Electrochemical cell lysis of gram-  
477 positive and gram-negative bacteria: DNA extraction from environmental water samples,  
478 *Electrochim. Acta.* 338 (2020) 135864. doi:10.1016/j.electacta.2020.135864.

479 [10] H. Yan, Y. Zhu, Y. Zhang, L. Wang, J. Chen, Y. Lu, Y. Xu, W. Xing, Multiplex detection  
480 of bacteria on an integrated centrifugal disk using bead-beating lysis and loop-mediated  
481 amplification, *Sci. Rep.* 7 (2017) 1–11. doi:10.1038/s41598-017-01415-x.

482 [11] V. Kamat, S. Pandey, K. Paknikar, D. Bodas, A facile one-step method for cell lysis and  
483 DNA extraction of waterborne pathogens using a microchip, *Biosens. Bioelectron.* 99  
484 (2018) 62–69. doi:10.1016/j.bios.2017.07.040.

485 [12] D. Taller, K. Richards, Z. Slouka, S. Senapati, R. Hill, D.B. Go, H.C. Chang, On-chip  
486 surface acoustic wave lysis and ion-exchange nanomembrane detection of exosomal RNA

487 for pancreatic cancer study and diagnosis, *Lab Chip.* 15 (2015) 1656–1666.  
488 doi:10.1039/c5lc00036j.

489 [13] S. Wang, X. Lv, Y. Su, Z. Fan, W. Fang, J. Duan, S. Zhang, B. Ma, F. Liu, H. Chen, Z.  
490 Geng, H. Liu, Piezoelectric Microchip for Cell Lysis through Cell–Microparticle Collision  
491 within a Microdroplet Driven by Surface Acoustic Wave Oscillation, *Small.* 15 (2019) 1–  
492 9. doi:10.1002/smll.201804593.

493 [14] C.M. Gabardo, A.M. Kwong, L. Soleymani, Rapidly prototyped multi-scale electrodes to  
494 minimize the voltage requirements for bacterial cell lysis, *Analyst.* 140 (2015) 1599–1608.  
495 doi:10.1039/c4an02150a.

496 [15] B.C. Gross, K.B. Anderson, J.E. Meisel, M.I. McNitt, D.M. Spence, Polymer Coatings in  
497 3D-Printed Fluidic Device Channels for Improved Cellular Adherence Prior to Electrical  
498 Lysis, *Anal. Chem.* 87 (2015) 6335–6341. doi:10.1021/acs.analchem.5b01202.

499 [16] H. Zhang, Y. Wang, Y. Zhou, K. Xu, N. Li, Q. Wen, Q. Yang, Aqueous biphasic systems  
500 containing PEG-based deep eutectic solvents for high-performance partitioning of RNA,  
501 *Talanta.* 170 (2017) 266–274. doi:10.1016/j.talanta.2017.04.018.

502 [17] P. Xu, Y. Wang, J. Chen, X. Wei, W. Xu, R. Ni, J. Meng, Y. Zhou, A novel aqueous  
503 biphasic system formed by deep eutectic solvent and ionic liquid for DNA partitioning,  
504 *Talanta.* 189 (2018) 467–479. doi:10.1016/j.talanta.2018.07.035.

505 [18] M. V Quental, A.Q. Pedro, P. Pereira, M. Sharma, J.A. Queiroz, J.A.P. Coutinho, F.  
506 Sousa, M.G. Freire, Integrated Extraction-Preservation Strategies for RNA Using  
507 Biobased Ionic Liquids, *ACS Sustain. Chem. Eng.* 7 (2019) 9439–9448.  
508 doi:10.1021/acssuschemeng.9b00688.

509 [19] S.F. Cheung, M.F. Yee, N.K. Le, B.M. Wu, D.T. Kamei, A one-pot, isothermal DNA  
510 sample preparation and amplification platform utilizing aqueous two-phase systems, *Anal.*  
511 *Bioanal. Chem.* 410 (2018) 5255–5263. doi:10.1007/s00216-018-1178-4.

512 [20] E.A. Frankel, P.C. Bevilacqua, C.D. Keating, Polyamine/Nucleotide Coacervates Provide  
513 Strong Compartmentalization of Mg<sup>2+</sup>, Nucleotides, and RNA, *Langmuir.* 32 (2016)  
514 2041–2049. doi:10.1021/acs.langmuir.5b04462.

515 [21] D. Mondal, A. Mahto, P. Veerababu, J. Bhatt, K. Prasad, S.K. Nataraj, Deep eutectic  
516 solvents as a new class of draw agent to enrich low abundance DNA and proteins using  
517 forward osmosis, *RSC Adv.* 5 (2015) 89539–89544. doi:10.1039/C5RA20735E.

518 [22] K.D. Clark, O. Nacham, H. Yu, T. Li, M.M. Yamsek, D.R. Ronning, J.L. Anderson,  
519 Extraction of DNA by magnetic ionic liquids: Tunable solvents for rapid and selective  
520 DNA analysis, *Anal. Chem.* 87 (2015) 1552–1559. doi:10.1021/ac504260t.

521 [23] M.N. Emaus, K.D. Clark, P. Hinnens, J.L. Anderson, Preconcentration of DNA using  
522 magnetic ionic liquids that are compatible with real-time PCR for rapid nucleic acid  
523 quantification, *Anal. Bioanal. Chem.* 410 (2018) 4135–4144.

524 [24] G. Günal, Ç. Kip, S. Eda Öğüt, H. İlhan, G. Kibar, A. Tuncel, Comparative DNA isolation  
525 behaviours of silica and polymer based sorbents in batch fashion: monodisperse silica  
526 microspheres with bimodal pore size distribution as a new sorbent for DNA isolation,

527 Artif. Cells, Nanomedicine Biotechnol. 1401 (2017) 1–7.  
 528 doi:10.1080/21691401.2017.1304404.

529 [25] D.S. Juang, S.M. Berry, C. Li, J.M. Lang, D.J. Beebe, Centrifugation-Assisted Immiscible  
 530 Fluid Filtration for Dual-Bioanalyte Extraction, *Anal. Chem.* 91 (2019) 11848–11855.  
 531 doi:10.1021/acs.analchem.9b02572.

532 [26] I.A. Nanayakkara, W. Cao, I.M. White, Simplifying Nucleic Acid Amplification from  
 533 Whole Blood with Direct Polymerase Chain Reaction on Chitosan Microparticles, *Anal.*  
 534 *Chem.* 89 (2017) 3773–3779. doi:10.1021/acs.analchem.7b00274.

535 [27] L.L. Hu, B. Hu, L.M. Shen, D.D. Zhang, X.W. Chen, J.H. Wang, Polyethyleneimine-iron  
 536 phosphate nanocomposite as a promising adsorbent for the isolation of DNA, *Talanta*. 132  
 537 (2015) 857–863. doi:10.1016/j.talanta.2014.10.047.

538 [28] Y. Haddad, K. Xhaxhiu, P. Kopel, D. Hynek, O. Zitka, V. Adam, The isolation of DNA  
 539 by polycharged magnetic particles: An analysis of the interaction by zeta potential and  
 540 particle size, *Int. J. Mol. Sci.* 17 (2016) 1–11. doi:10.3390/ijms17040550.

541 [29] Y. Bai, Y. Cui, G.C. Paoli, C. Shi, D. Wang, M. Zhou, L. Zhang, X. Shi, Synthesis of  
 542 amino-rich silica-coated magnetic nanoparticles for the efficient capture of DNA for PCR,  
 543 *Colloids Surfaces B Biointerfaces*. 145 (2016) 257–266.  
 544 doi:10.1016/j.colsurfb.2016.05.003.

545 [30] K. Xu, Y. Wang, H. Zhang, Q. Yang, X. Wei, P. Xu, Y. Zhou, Solid-phase extraction of  
 546 DNA by using a composite prepared from multiwalled carbon nanotubes, chitosan, Fe<sub>3</sub>O<sub>4</sub>  
 547 and a poly(ethylene glycol)-based deep eutectic solvent, *Microchim. Acta*. 184 (2017)  
 548 4133–4140. doi:10.1007/s00604-017-2444-4.

549 [31] M. Liu, X. Ding, X. Wang, J. Li, H. Yang, Y. Yin, Extraction of DNA from complex  
 550 biological sample matrices using guanidinium ionic liquid modified magnetic  
 551 nanocomposites, *RSC Adv.* 9 (2019) 23119–23128. doi:10.1039/c9ra01505a.

552 [32] J. Meng, Y. Wang, Y. Zhou, J. Chen, X. Wei, R. Ni, Z. Liu, F. Xu, A composite  
 553 consisting of a deep eutectic solvent and dispersed magnetic metal-organic framework  
 554 (type UiO-66-NH<sub>2</sub>) for solid-phase extraction of RNA, *Microchim. Acta*. 187 (2020).  
 555 doi:10.1007/s00604-019-4040-2.

556 [33] H. Yan, Y. Xu, Y. Lu, W. Xing, Reduced Graphene Oxide-Based Solid-Phase Extraction  
 557 for the Enrichment and Detection of microRNA, *Anal. Chem.* 89 (2017) 10137–10140.  
 558 doi:10.1021/acs.analchem.7b03138.

559 [34] O. Nacham, K.D. Clark, J.L. Anderson, Extraction and Purification of DNA from  
 560 Complex Biological Sample Matrices Using Solid-Phase Microextraction Coupled with  
 561 Real-Time PCR, *Anal. Chem.* 88 (2016) 7813–7820. doi:10.1021/acs.analchem.6b01861.

562 [35] O. Nacham, K.D. Clark, M. Varona, J.L. Anderson, Selective and Efficient RNA Analysis  
 563 by Solid-Phase Microextraction, *Anal. Chem.* 89 (2017) 10661–10666.  
 564 doi:10.1021/acs.analchem.7b02733.

565 [36] M. Varona, X. Ding, K.D. Clark, J.L. Anderson, Solid-Phase Microextraction of DNA  
 566 from Mycobacteria in Artificial Sputum Samples to Enable Visual Detection Using

567 Isothermal Amplification, *Anal. Chem.* 90 (2018) 6922–6928.  
568 doi:10.1021/acs.analchem.8b01160.

569 [37] M. Varona, D.R. Eitzmann, D. Pagariya, R.K. Anand, J.L. Anderson, Solid-Phase  
570 Microextraction Enables Isolation of BRAF V600E Circulating Tumor DNA from Human  
571 Plasma for Detection with a Molecular Beacon Loop-Mediated Isothermal Amplification  
572 Assay, *Anal. Chem.* 92 (2020) 3346–3353. doi:10.1021/acs.analchem.9b05323.

573 [38] R.N. Deraney, L. Schneider, A. Tripathi, Synergistic use of electroosmotic flow and  
574 magnetic forces for nucleic acid extraction, *Analyst*. 145 (2020) 2412–2419.  
575 doi:10.1039/c9an02191d.

576 [39] H. Zhang, F. Huang, G. Cai, Y. Li, J. Lin, Rapid and sensitive detection of *Escherichia*  
577 *coli* O157:H7 using coaxial channel-based DNA extraction and microfluidic PCR, *J.*  
578 *Dairy Sci.* 101 (2018) 9736–9746. doi:10.3168/jds.2018-14730.

579 [40] K. Perez-Toralla, I. Pereiro, S. Garrigou, F. Di Federico, C. Proudhon, F.C. Bidard, J.L.  
580 Viovy, V. Taly, S. Descroix, Microfluidic extraction and digital quantification of  
581 circulating cell-free DNA from serum, *Sensors Actuators, B Chem.* 286 (2019) 533–539.  
582 doi:10.1016/j.snb.2019.01.159.

583 [41] O. Strohmeier, S. Keil, B. Kanat, P. Patel, M. Niedrig, M. Weidmann, F. Hufert, J.  
584 Drexler, R. Zengerle, F. Von Stetten, Automated nucleic acid extraction from whole  
585 blood, *B. subtilis*, *E. coli*, and Rift Valley fever virus on a centrifugal microfluidic  
586 LabDisk, *RSC Adv.* 5 (2015) 32144–32150. doi:10.1039/c5ra03399c.

587 [42] D. Brassard, M. Geissler, M. Descarreaux, D. Tremblay, J. Daoud, L. Clime, M. Mounier,  
588 D. Charlebois, T. Veres, Extraction of nucleic acids from blood: unveiling the potential of  
589 active pneumatic pumping in centrifugal microfluidics for integration and automation of  
590 sample preparation processes, *Lab Chip.* 19 (2019) 1941–1952.  
591 doi:10.1039/C9LC00276F.

592 [43] W. Gan, Y. Gu, J. Han, C.X. Li, J. Sun, P. Liu, Chitosan-Modified Filter Paper for  
593 Nucleic Acid Extraction and “in Situ PCR” on a Thermoplastic Microchip, *Anal. Chem.*  
594 89 (2017) 3568–3575. doi:10.1021/acs.analchem.6b04882.

595 [44] C.E. Jin, T.Y. Lee, B. Koo, K.C. Choi, S. Chang, S.Y. Park, J.Y. Kim, S.H. Kim, Y. Shin,  
596 Use of Dimethyl Pimelimidate with Microfluidic System for Nucleic Acids Extraction  
597 without Electricity, *Anal. Chem.* 89 (2017) 7502–7510.  
598 doi:10.1021/acs.analchem.7b01193.

599 [45] A.S. Kastania, K. Tsougeni, G. Papadakis, E. Gizeli, G. Kokkoris, A. Tserepi, E.  
600 Gogolides, Plasma micro-nanotextured polymeric micromixer for DNA purification with  
601 high efficiency and dynamic range, *Anal. Chim. Acta*. 942 (2016) 58–67.  
602 doi:10.1016/j.aca.2016.09.007.

603 [46] N.M. Rodriguez, W.S. Wong, L. Liu, R. Dewar, C.M. Klapperich, A fully integrated  
604 paperfluidic molecular diagnostic chip for the extraction, amplification, and detection of  
605 nucleic acids from clinical samples, *Lab Chip.* 16 (2016) 753–763.  
606 doi:10.1039/C5LC01392E.

607 [47] C.-Y. Wen, T.-T. Liu, L.-L. Wu, Y.-M. Li, J.-Y. Sun, J.-B. Zeng, Magnetic nanospheres  
608 for convenient and efficient capture and release of hepatitis B virus DNA, *Talanta*. 197  
609 (2019) 605–611.

610 [48] P. Daggumati, S. Appelt, Z. Matharu, M.L. Marco, E. Seker, Sequence-Specific Electrical  
611 Purification of Nucleic Acids with Nanoporous Gold Electrodes, *J. Am. Chem. Soc.* 138  
612 (2016) 7711–7717. doi:10.1021/jacs.6b03563.

613 [49] D.C. Leslie, J. Li, B.C. Strachan, M.R. Begley, D. Finkler, L.A.L. Bazydlo, N.S. Barker,  
614 D.M. Haverstick, M. Utz, J.P. Landers, New detection modality for label-free  
615 quantification of DNA in biological samples via superparamagnetic bead aggregation, *J.*  
616 *Am. Chem. Soc.* 134 (2012) 5689–5696. doi:10.1021/ja300839n.

617 [50] H.S. Sloane, K.A. Kelly, J.P. Landers, Rapid KRAS Mutation Detection via  
618 Hybridization-Induced Aggregation of Microbeads, *Anal. Chem.* 87 (2015) 10275–10282.  
619 doi:10.1021/acs.analchem.5b01876.

620 [51] K.D. Clark, M. Varona, J.L. Anderson, Ion-Tagged Oligonucleotides Coupled with a  
621 Magnetic Liquid Support for the Sequence-Specific Capture of DNA, *Angew. Chemie -*  
622 *Int. Ed.* 56 (2017) 7630–7633. doi:10.1002/anie.201703299.

623 [52] T. Maruyama, T. Hosogi, M. Goto, Sequence-selective extraction of single-stranded DNA  
624 using DNA-functionalized reverse micelles, *Chem. Commun.* 43 (2007) 4450–4452.  
625 doi:10.1039/b708082d.

626 [53] T. Maruyama, N. Ishizu, Liquid–Liquid Extraction of Functional Single-Stranded DNA  
627 Using Reverse Micelles with DNA-Surfactant, *ChemNanoMat.* 2 (2016) 461–465.

628 [54] T. Maruyama, N. Ishizu, Y. Eguchi, T. Hosogi, M. Goto, Liquid–liquid extraction of  
629 enzymatically synthesized functional RNA oligonucleotides using reverse micelles with a  
630 DNA-surfactant, *Chem. Commun.* 52 (2016) 12376–12379.

631 [55] P. Scherp, K.H. Hasenstein, Solid phase gene extraction isolates mRNA at high spatial  
632 and temporal resolution, *Biotechniques.* 45 (2008) 172–178. doi:10.2144/000112831.

633 [56] M.R. Park, Y.H. Wang, K.H. Hasenstein, Profiling Gene Expression in Germinating  
634 Brassica Roots, *Plant Mol. Biol. Report.* 32 (2014) 541–548. doi:10.1007/s11105-013-  
635 0668-y.

636 [57] M.R. Park, K.H. Hasenstein, Hormone-Induced Gene Expression During Gravivcurvature  
637 of Brassica Roots, *J. Plant Growth Regul.* 35 (2016) 190–201. doi:10.1007/s00344-015-  
638 9518-5.

639 [58] G.G. Nestorova, K. Hasenstein, N. Nguyen, M.A. DeCoster, N.D. Crews, Lab-on-a-chip  
640 mRNA purification and reverse transcription via a solid-phase gene extraction technique,  
641 *Lab Chip.* 17 (2017) 1128–1136. doi:10.1039/c6lc01421f.

642 [59] W.M. Hanson, Z. Chen, L.K. Jackson, M. Attaf, A.K. Sewell, J.M. Heemstra, J.D.  
643 Phillips, Reversible Oligonucleotide Chain Blocking Enables Bead Capture and  
644 Amplification of T-Cell Receptor  $\alpha$  and  $\beta$  Chain mRNAs, *J. Am. Chem. Soc.* 138 (2016)  
645 11073–11076. doi:10.1021/jacs.6b04465.

646 [60] J. Kennedy-Darling, H. Guillen-Ahlers, M.R. Shortreed, M. Scalf, B.L. Frey, C.  
647 Kendziorski, M. Olivier, A.P. Gasch, L.M. Smith, Discovery of chromatin-associated  
648 proteins via sequence-specific capture and mass spectrometric protein identification in  
649 *saccharomyces cerevisiae*, *J. Proteome Res.* 13 (2014) 3810–3825.  
650 doi:10.1021/pr5004938.

651 [61] Y. Dai, J. Kennedy-Darling, M.R. Shortreed, M. Scalf, A.P. Gasch, L.M. Smith,  
652 Multiplexed Sequence-Specific Capture of Chromatin and Mass Spectrometric Discovery  
653 of Associated Proteins, *Anal. Chem.* 89 (2017) 7841–7846.  
654 doi:10.1021/acs.analchem.7b01784.

655 [62] M. Spiniello, R.A. Knoener, M.I. Steinbrink, B. Yang, A.J. Cesnik, K.E. Buxton, M.  
656 Scalf, D.F. Jarrard, L.M. Smith, HyPR-MS for Multiplexed Discovery of MALAT1,  
657 NEAT1, and NORAD lncRNA Protein Interactomes, *J. Proteome Res.* 17 (2018) 3022–  
658 3038. doi:10.1021/acs.jproteome.8b00189.

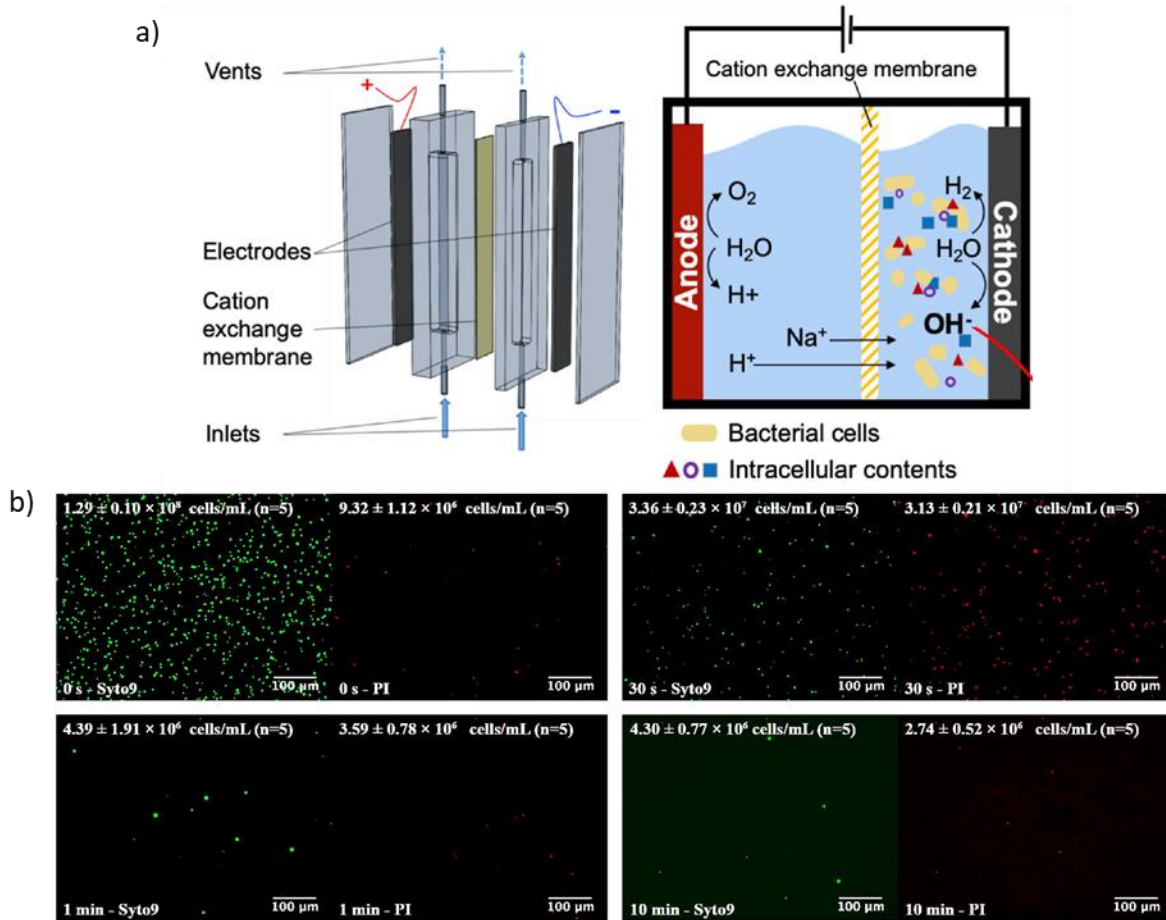
659

660

661

662

663



664

665 **Figure 1** (a) Schematic of the electrochemical device used to lyse waterborne pathogens. (b)  
666 Fluorescent monitoring of viable (green) and recently dead (red) *E. coli* cells during  
667 electrochemical lysis. Reproduced with permission from Ref. [9]

668

669

670

671

672

673

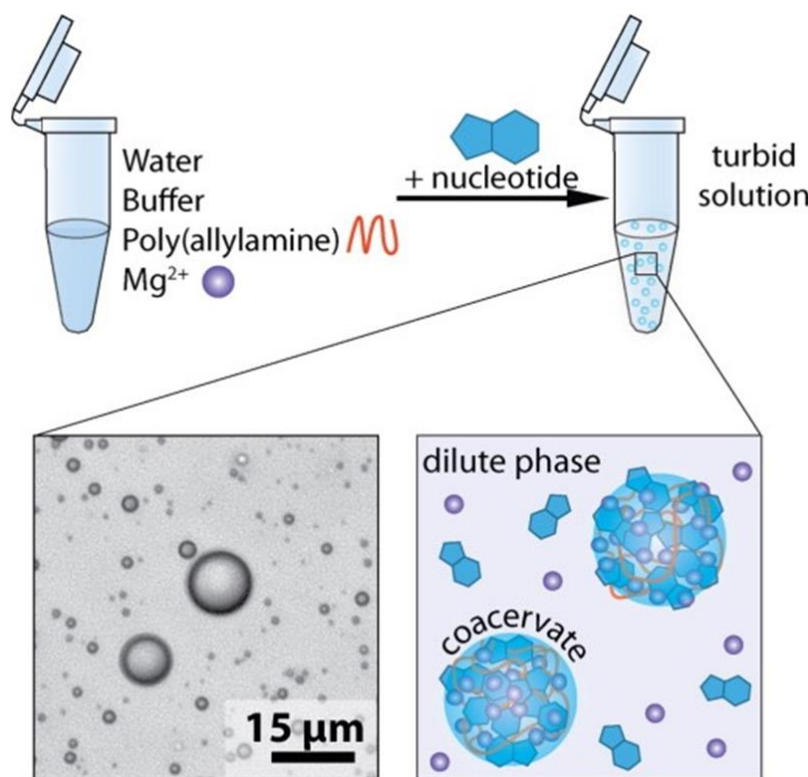
674

675

676

677

678



679

680

681 **Figure 2** Experimental approach for the formation of coacervates from electrolytes. Reproduced  
682 with permission from Ref. [20]

683

684

685

686

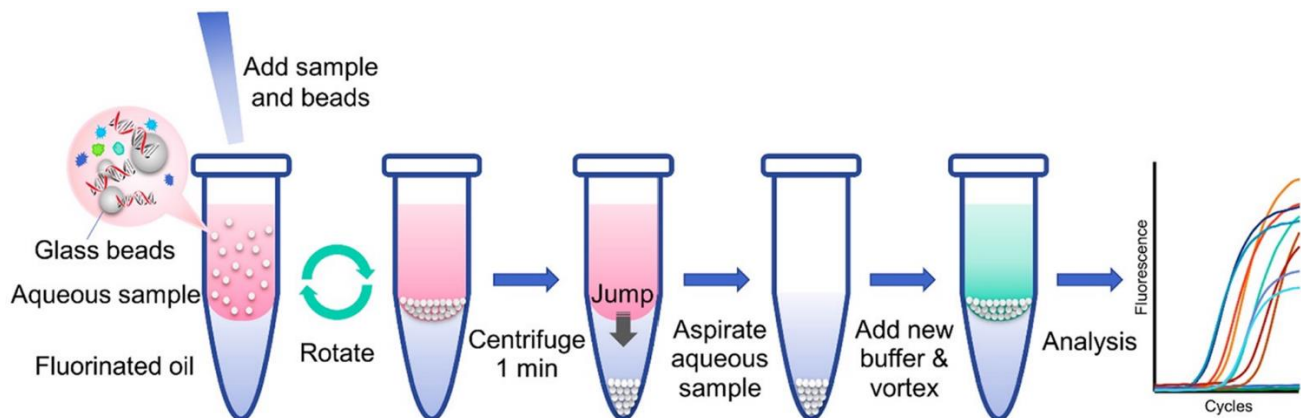
687

688

689

690

691



692

693 **Figure 3** NA extraction procedure using the CIFF method where NAs are adsorbed onto glass  
 694 beads then isolated from the sample matrix by being pelleted in a fluorinated oil. Reproduced with  
 695 permission from Ref. [25]

696

697

698

699

700

701

702

703

704

705

706

707

708

709

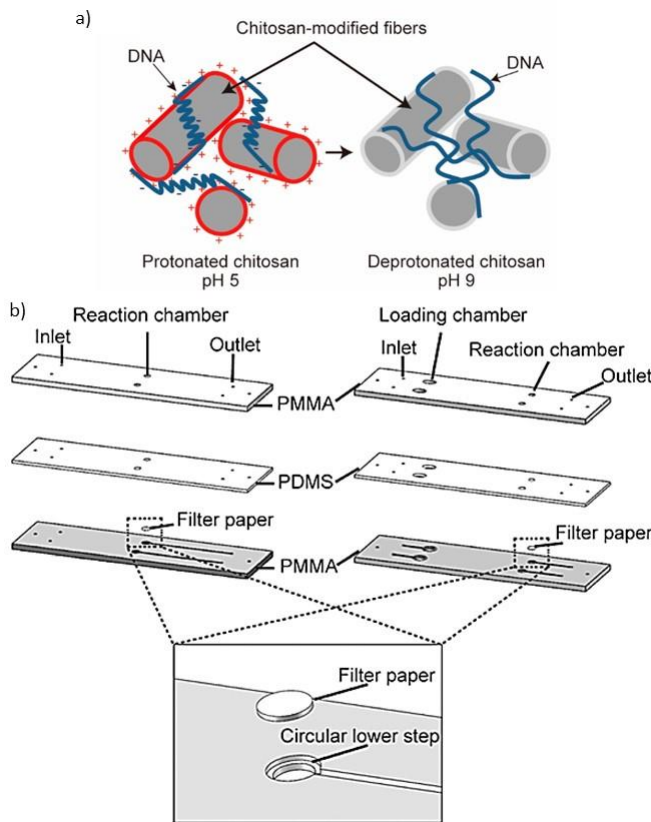
710

711

712

713

714



715

716 **Figure 4** a) DNA capture mechanisms using the chitosan-modified filter paper. b) Exploded view  
 717 of the microchips that contain a (left) single reaction chamber and (right) a sample loading and  
 718 reaction chamber used for DNA capture with the chitosan-modified filter paper. Reproduced with  
 719 permission from Ref. [43]

720

721

722

723

724

725

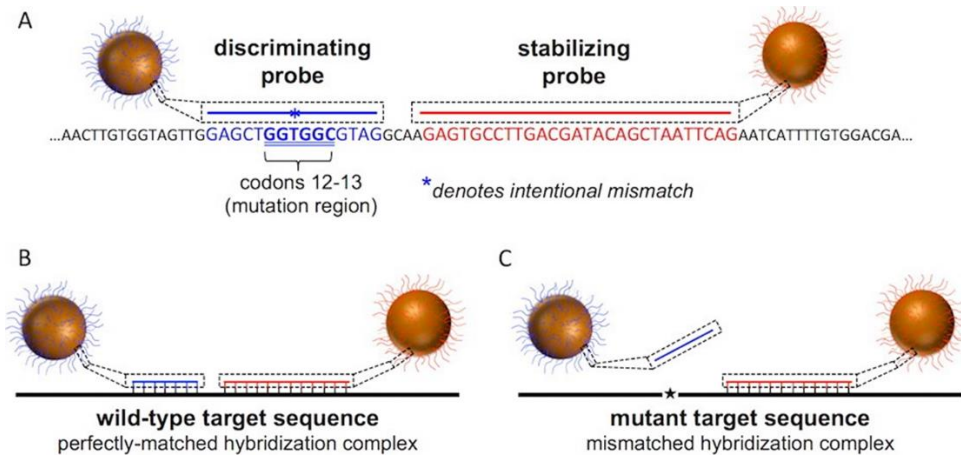
726

727

728

729

730



733 **Figure 5** (a) Design of the discriminating and stabilizing probes. (b) Both the stabilizing and  
 734 hybridization probe bind to the wild-type target causing visual aggregation. (c) Only the stabilizing  
 735 probe binds to the mutant target preventing aggregation. Reproduced with permission from Ref.  
 736 [50]